

SOUTHERN HEMISPHERE CYCLONE AND ANTICYCLONE BEHAVIOR DURING THE LAST DECADES: RECENT TRENDS, ANOMALIES AND LINKS WITH THE PACIFIC OCEAN VARIABILITY

Alexandre B. Pezza and Ian Simmonds
The University of Melbourne, Victoria, Australia

1. INTRODUCTION

The synoptic activity in the Southern Hemisphere, particularly extratropical cyclone and anticyclone behaviour, is strongly associated with climate variability in the Pacific Ocean. The most commonly known example of this association is the El Niño / Southern Oscillation (ENSO), which is one of the most studied interannual modes of variability in the climate system, with extensive discussion in the literature about its predictability and teleconnection effects on temperature and precipitation anomalies over the globe (Rasmusson and Carpenter 1982; Philander 1985; Cane et al 1986; Ropelewski and Halpert 1989; Karoly 1989; Smith and Stearns 1993; Hoerling et al 1997; Guo et al, 2004).

The term Pacific Decadal Oscillation (PDO) in connection with the ENSO-like pattern seen in lower frequencies of SST, pressure and other climate indicators was introduced by Mantua et al (1997), but a number of other studies (Zhang et al 1997 and references therein) have also pointed out the importance of such oscillation in the Pacific Ocean.

The PDO time variability is marked by an abrupt change towards a warmer tropical eastern Pacific and a colder extratropical central North Pacific in 1976-1977 (Zhang et al 1997; Mantua et al 1997) for reasons which are not yet fully comprehended.

It has been suggested, for example, that decadal large scale midlatitude anomalies in the atmospheric circulation over the Pacific basin may cause decadal modulation of the ENSO, through a teleconnection mechanism based on the projection onto the wind field overlying the equatorial regions (Barnett et al 1999), but it is not clear to what extent this would fully explain the observed variability reflected in the PDO index. On the other hand it has also been demonstrated that the El Niño is the leading mode for interdecadal variations (Karoly et al 1996), therefore placing a question on how much independence there is between the PDO and ENSO.

The PDO appears to have a much stronger signal in the extratropics if compared to the typical El Niño teleconnection mechanisms (Latif and Barnett 1994, Latif and Barnett, 1996, Mantua et al 1997, Zhang et al 1997). However, not much is known in terms of PDO impacts on the Southern Hemisphere extratropical climate and cyclone/anticyclone tracks, and to what extent the possible impacts would be significant.

Possible causes of the PDO and to which extent it would be fully predicted remains unsolved. Yasunaka and Hanawa (2005) for example argue that some of the important regime shifts occurred in global SSTs during the last century have happened concurrently with ENSO events, and suggest that decadal-scale variations and the ENSO events are not independent of each other, with the regime shifts being phase-locked in the ENSO events and the ENSO being phase-locked in the seasonal cycle of the climate system.

Each of these lines of research have been identified as high priority by the ongoing US CLIVAR

Corresponding authors address: Dr. Alexandre Bernardes Pezza. School of Earth Sciences, The University of Melbourne. Victoria 3010, Australia. E-mail: apezza@unimelb.edu.au.

program, as emphasised at recent international conferences as the 2005 CLIVAR/Argo meeting in Chile.

In this paper, we study the association between the PDO and the cyclone/anticyclone behavior in the Southern Hemisphere with an automatic tracking procedure developed at Melbourne University. Here we show that a coherent Hemispheric pattern of anomalies in different indicators of cyclone and anticyclone behaviour is found in association with the phase of the PDO index. This pattern is discussed in association with recent trends in cyclone/anticyclone activity and in light of the major PDO shift occurred in the mid seventies. Possible links with important features of the Southern Hemisphere synoptic climatology such as possible interactions with the Southern Annular Mode (SAM) and with extreme synoptic events such as polar air outbreaks are also discussed.

2. METHODOLOGY

We used monthly PDO index as described in Mantua et al (1997), i.e., derived as the leading Principal Component (PC) mode of monthly SST anomalies in the North Pacific Ocean, poleward of 20°N. The monthly mean global average SST anomalies were removed in an attempt to eliminate any possible signal associated with global warming. The index was obtained through the Joint Institute for the Study of the Atmosphere and Oceans at the University of Washington, for the period of 1900 – 2005 (<http://jisao.washington.edu>). The monthly SOI data was obtained from the Bureau of Meteorology in Australia, for the period of 1876 – 2005 (www.bom.gov.au).

Finally, monthly data for the Antarctic Oscillation Index (AAO) produced by NOAA for the period 1979 – 2005 was also used (www.cpc.ncep.noaa.gov) in an attempt to assess possible correlations between the Southern Annular Mode (SAM) and the PDO.

The Melbourne University automatic tracking scheme (Murray and Simmonds, 1991a,b) was used to calculate the cyclone and anticyclone trajectories and their statistical properties. This algorithm utilizes a totally automatic approach for locating low and high pressure centres on a sphere and calculating the trajectories. The scheme was chosen because of its proven reliability in capturing very well the weather patterns and synoptic climatology of the transient activity in the Southern Hemisphere (Jones and Simmonds, 1993, 1994; Simmonds et al, 1999, Simmonds and Keay, 2000 a, b; Pezza and Ambrizzi 2003, 2005), and because it deals directly with sea level pressure, giving a synoptic meaning to the analyses.

The statistical component of the software comprises a series of calculations based on estimated physical properties such as radius, Laplacian of the pressure, velocity of displacement, and others. The most important variables calculated in terms of spatial distribution and used in this work are the System Density (SD) and the Depth (DP). The first is defined as the number of cyclones/anticyclones in a reference area of 10^3 (deg. lat)², whereas the second is the pressure difference between the edge and the centre of a given system (Simmonds et al 2003). The radius and the Depth are related by (1):

$$D = 0.25 R^2 \nabla^2(P) \quad (1)$$

The tracks and statistical properties were calculated based on the mean sea level pressure (MSLP) derived from the European Centre for Medium-Range Weather Forecasts (ECMWF) reanalysis - ERA 40 (Uppala et al 2006), for the period 1957-2002.

Composites of MSLP, trajectories, system density and Depth were calculated for the positive and negative phases of the PDO and SOI, considering only the cases above the average plus one standard deviation or below the average minus one standard deviation. All anomalies related to cyclone/anticyclone

properties were calculated based on the ERA40 climatology for the whole period available. The analyses have been performed on a seasonal basis, but here we show anomalies of cyclone and anticyclone behavior only for the winter season, when the influence of migratory cyclone/anticyclone activity at midlatitudes is at its maximum.

3. RESULTS AND DISCUSSION

The years in which the PDO and SOI indices were above the average plus one standard deviation (+) and below the average minus one standard deviation (-) are shown in Table 1 for each season for the 1957-2002 reference period which coincides with the ERA40 climatology. Cases of “coincident” PDO⁺ with SOI⁻ and PDO⁻ with SOI⁺ are respectively shown in red and blue, and cases of PDO and SOI having the same signal are shown in green.

From this table it can be seen that, as expected, a significant percentage of El Niño conditions tend to occur during the positive phase of the PDO, whereas a significant percentage of La Niña years occur during the negative phase of the PDO.

On an annual basis, 50% of the El Niño and 56% of the La Niña conditions were accompanied by the coincident PDO phase. On the other hand, in terms of PDO and SOI having the same signal (opposite phases), this happened only for the spring of 1994 (in green), suggesting that such a combination is an extremely rare occurrence.

PDO/SOI phase	Years
Winter	
PDO ⁺	83, 87, 92, 93, 97
SOI ⁻	65, 72, 77, 82, 87, 93, 94, 97
PDO ⁻	61, 62, 63, 67, 71, 73, 75, 99
SOI ⁺	64, 73, 75, 81, 88, 96, 98
Summer	

PDO ⁺	77, 84, 85, 86, 87, 88, 94, 98
SOI ⁻	59, 73, 78, 83, 87, 1992, 98
PDO ⁻	62, 65, 69, 71, 72, 74, 76, 91, 00
SOI ⁺	62, 71, 74, 76, 89, 99, 00, 01
Autumn	
PDO ⁺	80, 81, 83, 84, 86, 87, 93, 96, 98
SOI ⁻	83, 87, 91, 92, 93, 94, 97, 98
PDO ⁻	62, 64, 67, 71, 72, 75, 76
SOI ⁺	64, 71, 74, 75, 89, 99, 00
Spring	
PDO ⁺	57, 76, 83, 86, 87, 92, 93, 97
SOI ⁻	65, 72, 77, 1982, 91, 94, 97
PDO ⁻	61, 62, 70, 73, 75, 94, 99, 01
SOI ⁺	64, 70, 71, 73, 75, 88, 98, 00
Annual	
PDO ⁺	81, 83, 84, 86, 87, 92, 93, 97
SOI ⁻	65, 77, 82, 83, 87, 91, 92, 93, 94, 97
PDO ⁻	61, 62, 64, 71, 72, 73, 75, 99
SOI ⁺	64, 71, 73, 74, 75, 88, 89, 99, 00

Table 1: Years used for the PDO and SOI composites, where (+) applies for the cases where the index was above the average plus one standard deviation, and (-) for cases below the climatological average minus one standard deviation. The PDO index from the Joint Institute for the Study of the Atmosphere and Oceans at the University of Washington and SOI from the Australian Bureau of Meteorology were used for the ERA40 1957-2002 reference period. Years of coincident phase, i.e., negative SOI with positive PDO or positive SOI with negative PDO are indicated in red for El Niño conditions and in blue for La Niña, and years of PDO and SOI with the same sign are in green. See text for more details.

Figure 1 shows the SST (shaded) and MSLP anomalies (contour) associated with the positive phase of the PDO index (upper panel) and with the positive phase of the cold tongue index (lower panel), which is the oceanic equivalent of the SOI index (after Mantua et al 1997). From this figure, it is observed

that the PDO index shows a SST signature which strongly resembles the typical ENSO pattern, however with amplified anomalies in the extratropics. This feature is also seen in the MSLP anomalies, which are much more pronounced in the extratropics in association with the PDO. Although the PDO index was defined as the PC of SST anomalies to the North of 20°N, it is associated with strong and organised anomalies of SST and MSLP over the SH. This, in turn, reflects the potential for the interaction of the PDO and SH synoptic behavior.

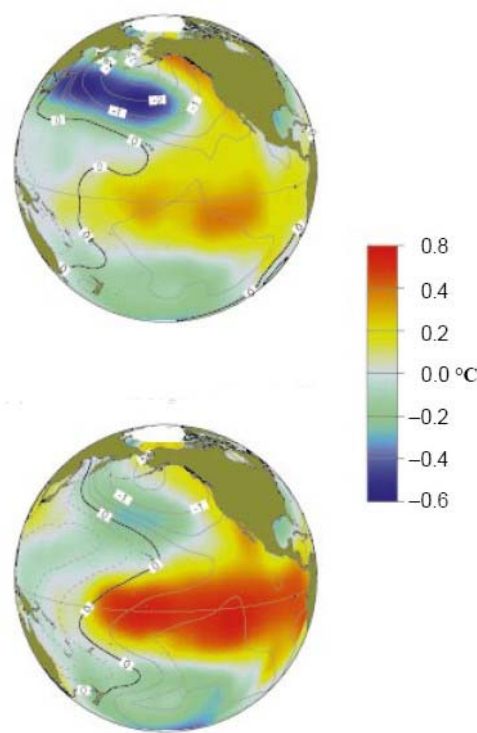


Figure 1: Sea surface temperature (color shaded) and mean sea level pressure (contoured) regressed upon the PDO index (upper panel) and the cold tongue index (lower panel) for the period 1900-1992. From Mantua et al (1997).

Figure 2 shows the historical behavior of the monthly PDO index (left hand scale) since the start of measured SST data in the beginning of the last century. The extreme minimum temperatures below 1° C for São Paulo in southeastern Brazil (23°S, 46°W, 799m), are also shown (right hand scale).

The meteorological station of the University of São Paulo has one the most reliable long term time series in South America and is strategically located in an area where the propagation of frontal systems is also influenced by the equatorial SSTs in the Pacific Ocean (Pezza and Ambrizzi 2005 and references therein).

The time series of the PDO index reflects the observed inter-decadal variability during the last century, with the last period corresponding to a persistent warm phase from 1977 to the present. A sudden reversal back to the negative phase in the year 2000 suggested that another major shift might be occurring, but this was quickly replaced by a strong positive signal after 2000. The last cold phase can be estimated as lasting between 1947 and 1976, preceded by a generally warm phase between 1925 and 1946 and finally by a somewhat mixed signal in the beginning of the last century.

The main PDO shift back to a positive phase which occurred in the mid-seventies appears at least partially in phase with a climate shift mainly evidenced in precipitation over midlatitude regions in South America, Africa and Australia, but the hypothesis of a possible physical link has not been demonstrated (Baines, 2005).

In terms of propagation of synoptic systems, it has been noted for example that winter time polar air outbreaks in subtropical South America tend to be more frequent during La Nina events (Rusticucci and Vargas, 2002), but to what extent a similar association may be also present in terms of the decadal variability in the Pacific is still unresolved.

The minimum temperatures in São Paulo presented in figure 2 reflect exceptional large scale synoptic conditions associated with a very pronounced meridional air exchange over a large area (Pezza and Ambrizzi 2005). The figure shows that strong cold incursions do occur during both phases of the PDO. One of the most intense events ever to

affect South America occurred in July 1976 just prior to the main phase shift occurred later in 1977. The absence of significant polar outbreaks in the 1980s coincided with a period of significant uninterrupted predominance of the positive phase, and the recent extreme cold outbreak of the year 2000 (minimum temperature below zero in figure 1) took place during a period when the PDO index became suddenly negative despite of being inside a major warm phase. However, in general terms no apparent correlation could be found between both parameters.

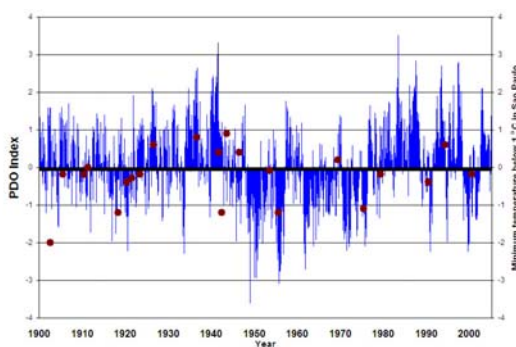


Figure 2: Monthly series of the PDO index (left scale) and minimum temperatures below 1.0°C in São Paulo (right scale) during 1900-2005.

On the other hand the average detrended annual temperature anomalies for the period 1934 – 2002 at the same station and the annual PDO index show a modest positive correlation, as seen in figure 3, hence suggesting at least the possibility of a small influence. This will be clearer for the analysis of cyclone/anticyclone behaviour discussed in the next paragraphs.

The association between the PDO and the SOI and the SAM was also explored. Figure 4 shows a linear regression between the monthly SOI and the PDO indices for the period of 1900 - 2005. From this figure, a clear negative association is seen between SOI and PDO, which was expected as discussed before. However, the strength of the linear relationship is relatively weak, with only about 10% of the overall variance being explained by the linear regression. This is not surprising given that the

variability of the ENSO and the PDO occur mainly at different time scales, and it may also be reflecting a certain degree of independency between both variables.

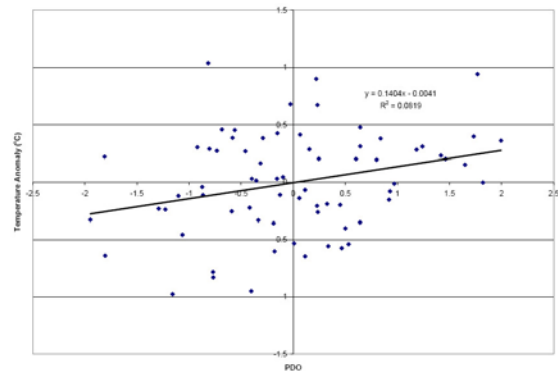


Figure 3: Detrended annual minimum temperature anomalies in São Paulo versus the PDO index for the period 1934 – 2002.

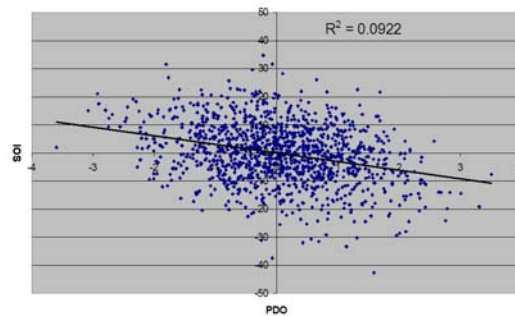


Figure 4: Linear regression between the monthly SOI and PDO indices during 1979 – 2005.

Figure 5 shows the linear regression between the monthly AAO and the PDO indices for January (upper panel) and September (lower panel) 1979 - 2004. It shows a moderate tendency for a negative relationship during the summer, what is in agreement with recent works (Carvalho et al 2005 and references therein). Interestingly this relationship between the SAM and the PDO during the summer is stronger than the relationship between the SAM and the SOI recently documented (Meneguini et al 2006), which may be indicative of a more annular structure of the PDO or, in other words, it may also be suggestive of a stronger extratropical response connected with

the PDO. This is therefore suggestive of the PDO having an influence on the storm track circulation around Antarctica.

An opposite influence is seen during the spring, with a very weak positive correlation between two variables. Interestingly it has been noted that the SOI and the AAO are also very weakly correlated during that time of the year (Meneguini et al 2006).

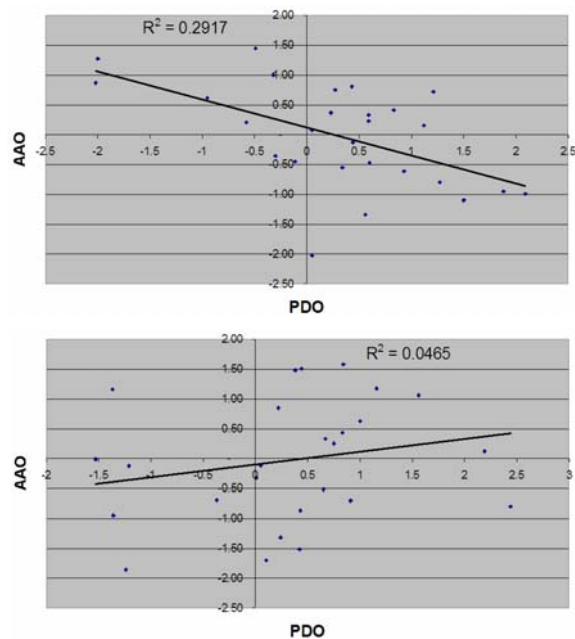


Figure 5: Linear regression between the monthly AAO and PDO indices during January (upper panel) and September (lower panel) 1979 – 2005.

Figure 6 shows the annual mean sea level pressure for (a) the PDO⁺ - PDO⁻ and (b) the SOI⁻ - SOI⁺ composites. It can be seen that although the patterns have a similar structure, significant differences can be found. The pressure tends to be higher in the eastern Hemisphere when the PDO is in the positive phase and the ENSO corresponds to the El Nino phase, with a marked maximum over Australia which is stronger for the SOI composite.

Over the western Hemisphere there is a broad area of below average pressure over the Pacific Ocean particularly for the SOI composite (figure 6b), indicating that the pressure found on that area during

El Nino events is significantly lower. This is also seen for the PDO composite (figure 6a) to a lesser extent.

In terms of differences, the most striking feature in figure 6 is that the PDO shows a much stronger annular pattern around Antarctica (figure 6a) if compared to the SOI response (figure 6b). This difference is significant, with a magnitude of several hPa. This is in agreement with the previous results, proposing a physical meaning for the correlations shown in figure 5, and is significant given the total amount of years used in the composites, i.e., 24 years for the PDO and 21 years for the SOI.

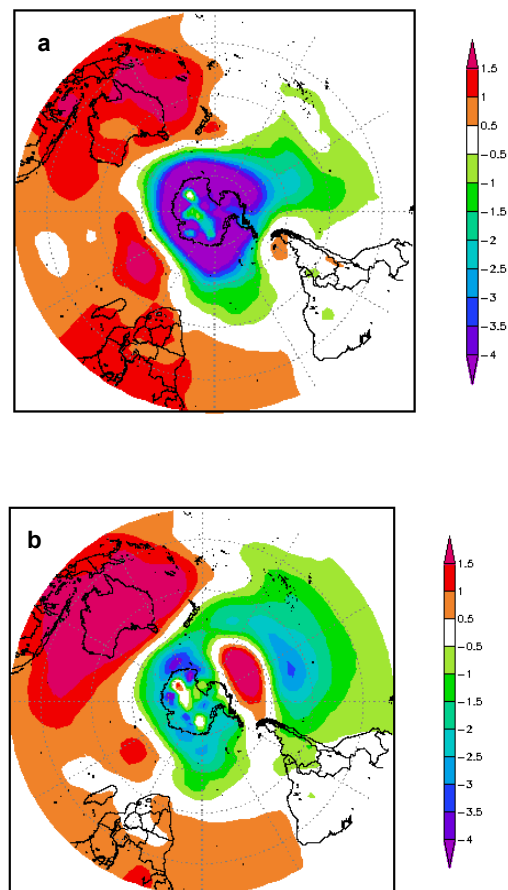


Figure 6: Annual mean sea level pressure anomalies for (a) PDO⁺ - PDO⁻ and (b) SOI⁻ - SOI⁺ for the period 1948 – 2004. Total number of years used in the composite: PDO⁺ 9 years, PDO⁻ 15 years, SOI⁺ 10 years, SOI⁻ 11 years.

Another substantial difference concerns the well known blocking high to the southwest of South America associated with El Nino conditions (Renwick 1998), which is clearly seen in the SOI composite but does not appear in the PDO case.

Figure 7 shows the wintertime (JJA) synoptic climatology of all (a) cyclone and (b) anticyclone tracks lasting more than 24 hours superposed on the same map for every six hours, for both phases of the PDO. The tracks which occurred during the PDO⁺ (PDO⁻) phase are shown in red (blue). Regions where tracks were found during the both phases are shown in green. No pressure restriction was applied, allowing for the inclusion of weak systems over the subtropical ridge and low latitudes.

Although the green area is showing the high density regions crossed by cyclones and anticyclones during both phases of the PDO from a climatological point of view, it does not necessarily mean that significant differences can not be found. This is given in terms of the SD and DP, discussed in the following paragraphs.

However, the trajectories in red and blue denote systems being tracked only during one particular phase. For example, this is the case of more cyclones in the equatorial western Pacific and Indian Ocean (in red) during the PDO⁺ and more cyclones in subtropical latitudes during the PDO⁻ (in blue) as seen in figure 7a, and more anticyclones over high latitudes during the PDO⁺ (figure 7b).

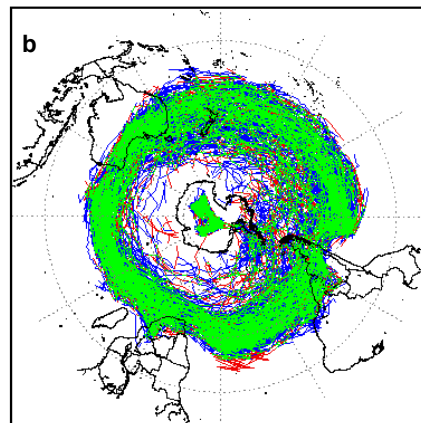
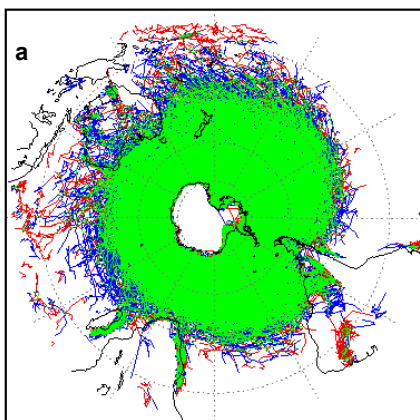


Figure 7: Superposed (a) cyclone and (b) anticyclone tracks for JJA PDO⁺ and PDO⁻ composites. The tracks which occurred only during the PDO⁺ (PDO⁻) phase are shown in red (blue). Regions where tracks were found during the both phases are shown in green. Tracks had to be at least 24 hours long to be considered. See text for more details.

Figure 8 shows the ERA40 climatology of the cyclone System Density (a) and Depth (b) as given by the Melbourne University automatic tracking scheme, and figure 9 is similar but for the anticyclones. From this figure it can be observed that the cyclones present a maximum density around Antarctica, with a typical magnitude between 6 and 10 SD units. The SD rapidly decreases towards lower latitudes. The DP presents a somewhat similar pattern, but it is worth noting that the maximum climatological DP areas do not necessarily occur over the maximum SD regions.

In terms of the anticyclones, a completely different pattern is seen, as demonstrated by figure 9. The regions of more intense DP are located over midlatitudes around the hemisphere, with maxima around the semi-permanent subtropical high pressure centers over the oceans. The strongest climatological SD in anywhere over a continent is located in southeastern Australia (Antarctica excepted). On the other hand the DP shows a maximum further south at mid-to-high latitudes, particularly over the south Pacific ocean in an area where the anticyclone activity is of crucial importance for the generation and

propagation of polar air outbreaks (Pezza and Ambrizzi 2005).

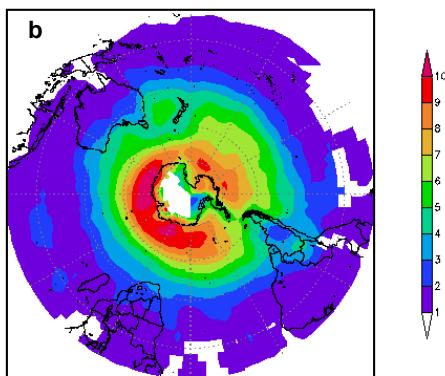
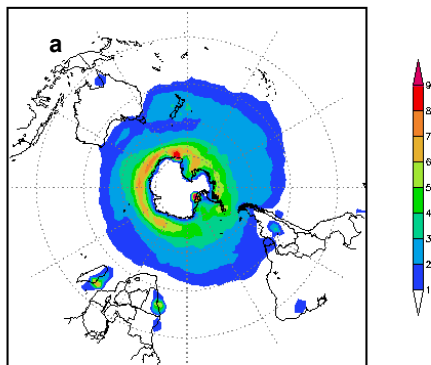


Figure 8: ERA40 climatology of cyclone SD (a) and DP (b) for the period 1957-2002, using the Melbourne University tracking scheme.

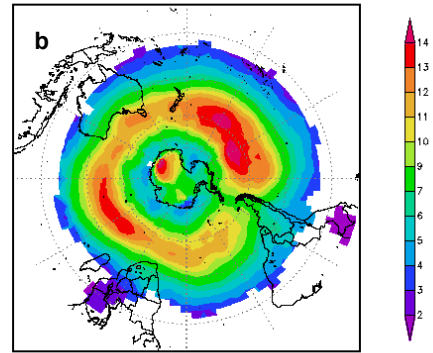
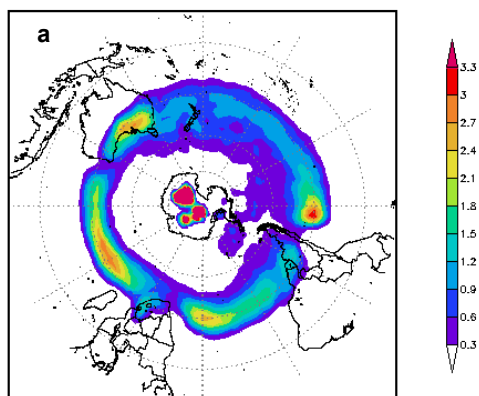


Figure 9: ERA40 climatology of anticyclone SD (a) and DP (b) for the period 1957-2002, using the Melbourne University tracking scheme.

Figure 10 shows the wintertime (JJA) System Density (SD) anomalies associated with the negative (upper panel) and positive (lower panel) phases of the PDO (PDO⁻ and PDO⁺ respectively).

The general SD pattern observed over the Southern Ocean and mid-to-high latitudes in figure 10 shows densities typically above average during the negative phase and below average during the positive phase of the PDO. This is in agreement with more cyclones appearing in blue over midlatitudes in figure 7a. Close to the Antarctic coast a different pattern is observed, with strong anomalies of opposite sign in the Ross and Weddell Seas, suggesting an intense dipole over that area. As seen in figure 6, that region of the globe presents a very interesting difference in terms of the pressure pattern comparing the PDO and the SOI composites, being apparently more responsive to the PDO phase.

The typical order of magnitude for the anomalies seen in figure 10 is about 1 SD unit for most of the midlatitudes, indicating an increase (or decrease) of up to 100% of the climatology for some cases as for example in the case of negative anomalies to the south of Australia during the positive phase of the PDO, and therefore being significant and giving physical meaning to the analyses. The stronger anomalies found over high latitudes around Antarctica

may be less representative in terms of the percentage of the climatology, given the typical very high SD found over the region, but they are still significant.

DP is above 1hPa for the most important anomalies over mid and high latitudes, where the climatological DP typically ranges between 4 and 10 hPa as seen in figure 8b.

When this is analysed together with the SD shown in figure 10, there is suggestion that in general terms the negative phase of the PDO is associated with more numerous but less intense cyclones, whereas the positive phase is associated with less but more intense cyclones. However, this combination is not seen in all regions. The Tasman Sea in the eastern coast of Australia, for instance, presents more numerous and stronger cyclones during the negative phase, and the coast of south Brazil presents more numerous and more intense cyclones during the positive phase.

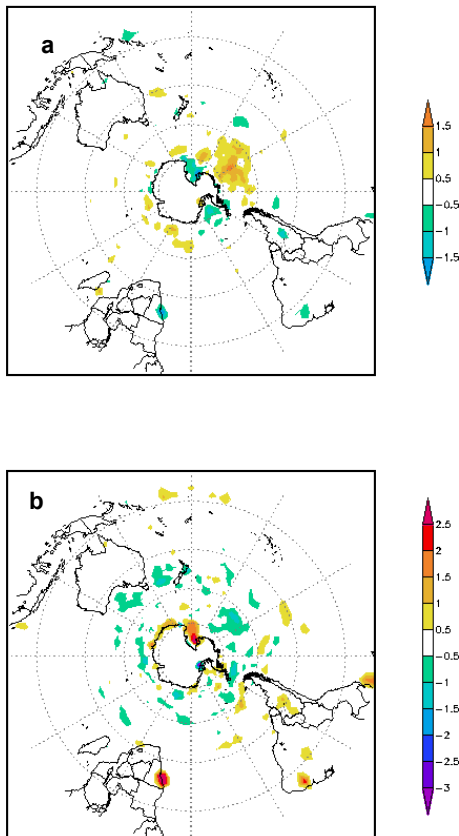


Figure 10: Cyclone SD (System Density) anomaly for the (upper) PDO⁻ and (lower) PDO⁺ composites during the winter season (JJA). The unit is given in SD units, i.e., number of cyclones $\times (10^3/\text{deg.lat}^2)$.

The corresponding DP anomalies are seen in figure 11, where a well marked pattern can be observed, with below average DP during the negative phase and above average values during the positive PDO composite. This is seen over much of the SH, and is suggestive of a well defined large scale pattern indicating that the cyclone strength tends to be very responsive to the PDO phase in a close to linear manner. The typical magnitude found for the cyclone

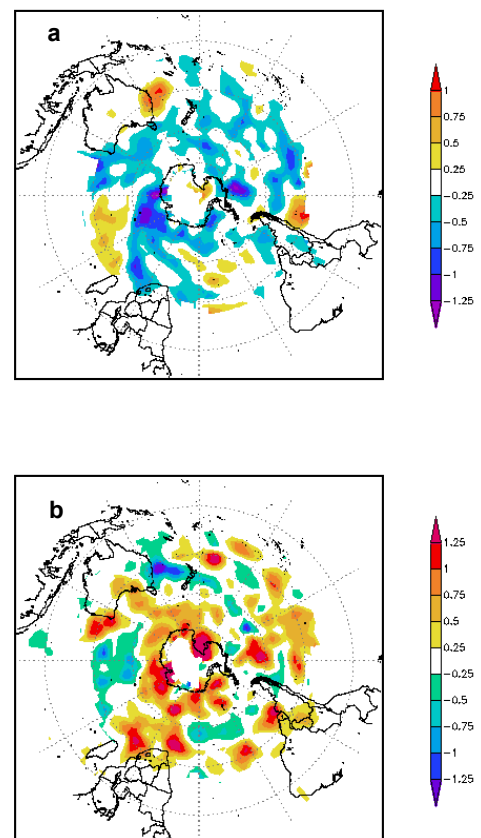


Figure 11: Cyclone DP (Depth) anomaly for the (upper) PDO⁻ and (lower) PDO⁺ composites during the winter season (JJA).

The Student's t-test (Wilks 1995) was applied, and it showed a pattern with values significantly different from zero with a confidence of at least 90% and up to 99% or above for the most intense anomalous centres. This was found for both SD and DP, and it was observed that a similar spatial pattern tends to be observed in all cases, with the significance contour lines roughly following the contours of the anomalies, especially for the DP maps.

Figures 12 and 13 show the SD and the DP similarly to figures 10 and 11, but for the anticyclone tracks. Figure 12 shows that the anticyclone SD anomalies present a stronger signal over midlatitudes if compared to the cyclone SD discussed for figure 10.

This is expected due to the typical spatial distribution of cyclones and anticyclones as seen in figure 7. The order of magnitude of the anticyclone SD anomalies is comparable to that of the cyclones, reaching values above 1 SD unit over some regions, which is significant when compared to the climatology.

In terms of the differences between the positive and negative phases of the PDO, figure 12 suggests predominantly positive anomalies for the PDO⁻ and negative anomalies for the PDO⁺, similarly to what was shown for the cyclones (figure 10) but apparently subject to a higher variability.

It is also notable from figure 12 that the south-eastern Pacific to the south-western of South America appears with strong positive anomalies during the negative phase and negative anomalies during the positive phase. This is a key area for polar outbreaks affecting South America, and the observed pattern is consistent with the idea of a reinforcement of the climatological propagation of anticyclones when we are in the negative phase of the PDO.

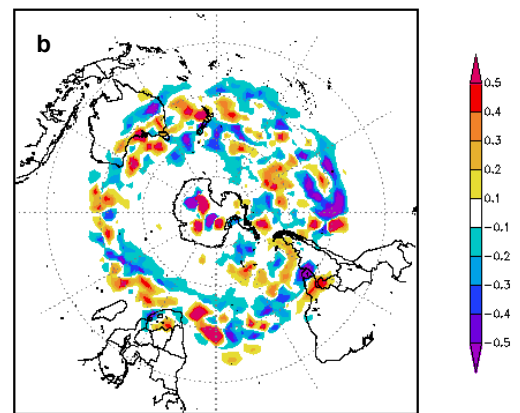
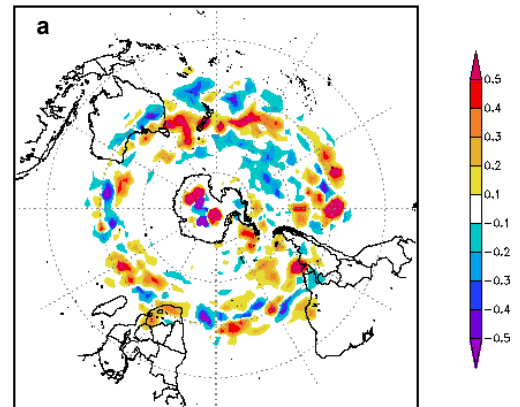
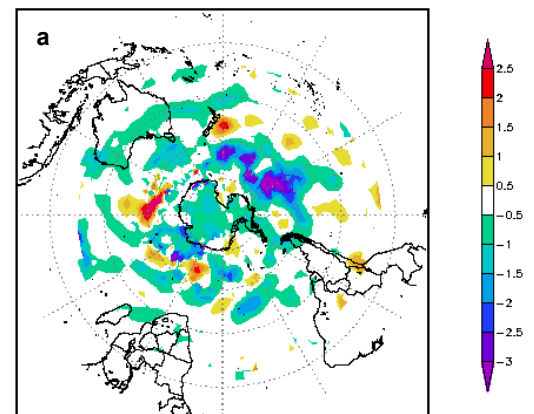


Figure 12: Anticyclone SD (System Density) anomaly for the (upper) PDO⁻ and (lower) PDO⁺ composites during the winter season (JJA).



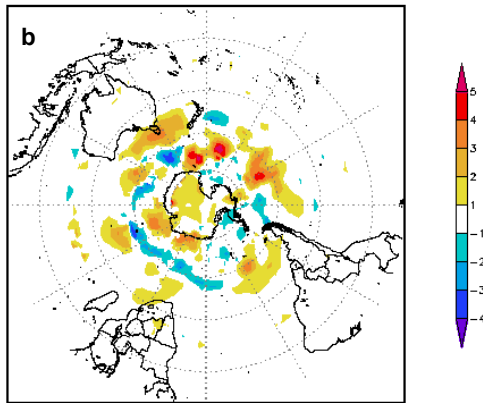


Figure 13: Anticyclone DP (Depth) anomaly for the (upper) PDO^- and (lower) PDO^+ composites during the winter season (JJA).

The anticyclone winter anomalous Depth patterns tend to be more uniform over the hemisphere, as seen in figure 13. In this case there is a consistent pattern indicating below average depth for the PDO^- composite and above average for the PDO^+ , similar to what was observed for the cyclones. The typical magnitude found over mid-to-high latitudes can be significantly strong, with anomalies above 5 hPa in some cases, representing up of 50% of the climatological strength over those latitudes.

The Southern Ocean between Australia and South America, for instance, presents consistent negative anomalies stronger than -3 hPa for the PDO^- and positive anomalies stronger than 5 hPa for the PDO^+ . This means a difference of the order of 10 hPa between the both extremes of PDO, which is strong compared to the climatology. The Student's t-test shows that the differences over this area are marginally significant at the 90% level.

In accordance to what was discussed for the anticyclone SD anomalies, this is a key area for the propagation of wave trains associated with polar air outbreaks over South America. A comparison between figures 12 and 13 for this sector suggests a possible link with slightly positive DP anomalies between New Zealand and South America around

35S during the PDO^- , which is also seen in terms of SD as discussed before. The strong negative Depth anomalies further south in this case may be a reflection of possible trajectories further north, leading to a coherent pattern of propagation when the PDO is negative. On the other hand, when the PDO is positive the DP anomalies suggest that the connection between Australia and South America seems to occur at higher latitudes (around 50°S), with positive anomalies also appearing on the Patagonian coast of Argentina at mid-to-high latitudes.

The influences discussed above are very important for the circulation of the Southern Hemisphere, and may impact important synoptic features such as rain and temperature anomalies over key areas and mechanisms associated with extreme events such as polar air outbreaks in South America. Although the anomalies discussed here can not be purely explained by the PDO, the consistency of some of the patterns found is surprising.

Figure 14 shows the trends in winter cyclones and anticyclones for the whole Southern Hemisphere between 1973 and 1996 given by the tracking scheme considering all pressure ranges (upper panel) and only for the most intense end of the spectrum given by cyclones below 980 hPa and anticyclones above 1035 hPa. It is interesting to see that there is a significant decrease in the total count of both winter cyclones and anticyclones when all pressure ranges are considered, but on the other hand the most intense cyclones seem to be increasing.

Figure 15 shows that this transition is gradual, with the count for all cyclones below 1000 hPa being in the middle between a positive trend for more intense systems and a negative trend for weaker systems.

Comparing the trends shown in figures 14 and 15 with the PDO pattern shown in figure 2 it can be seen that the cyclone trends for different pressure thresholds seem to have presented a shift which is

approximately coincident with the PDO shift occurred in the mid to late seventies.

The analysis of cyclone trends and PDO time series alone is suggestive of less but more intense cyclones during a period of positive PDO. It is therefore very interesting to note that this independent evidence is in agreement with the results discussed in figures 10 and 11 which clearly suggest negative winter cyclone SD anomalies (figure 10b) and very significant positive winter cyclone DP anomalies during the PDO+ composite.

Figure 16 summarizes the possible association between the PDO and polar air outbreaks in South America, adapted from the model produced by Pezza and Ambrizzi 2005. The SD and DP anomalies observed suggest that a reinforcement of the migratory anticyclones over the South Pacific between New Zealand and South America may generate conditions favorable to the enhancement of cold air outbreaks when the PDO is in its negative phase, whereas during the positive phase more numerous and stronger cyclones may be expected on the southern tip of the Brazilian coast, indicating the possibility of positive rainfall anomalies over the area.

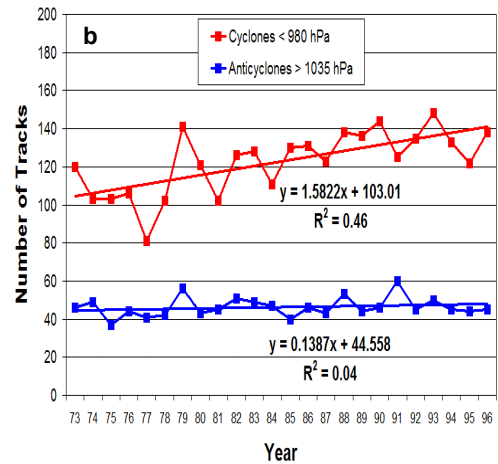
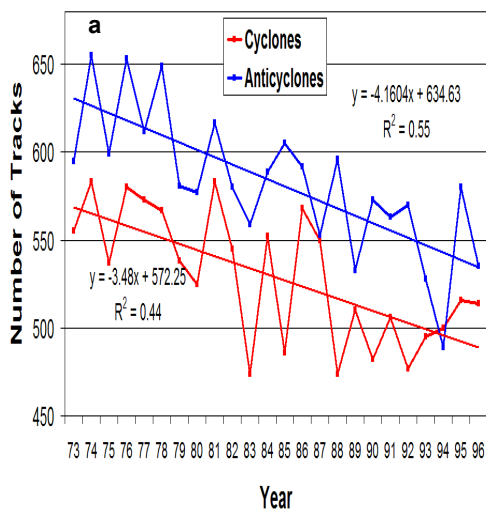


Figure 14: Number of cyclone and anticyclone tracks every 12h during JJA (1973-1996) for the whole SH (a) without pressure restriction and (b) for cyclones below 980 hPa and anticyclones above 1035 hPa. After Pezza and Ambrizzi (2003).

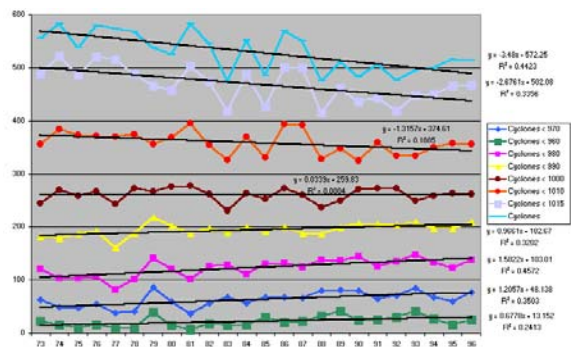


Figure 15: Number of cyclone tracks every 12h during JJA (1973-1996) for different pressure thresholds.

Although this is still speculative and more research is needed, this is an example of a possible physical link between the PDO and the high latitude circulation, and helps to explain the positive correlation between the PDO and the annual average temperatures in São Paulo and the fact that the most recent known strong polar outbreak was associated with a sudden shift of the PDO back to the negative phase.

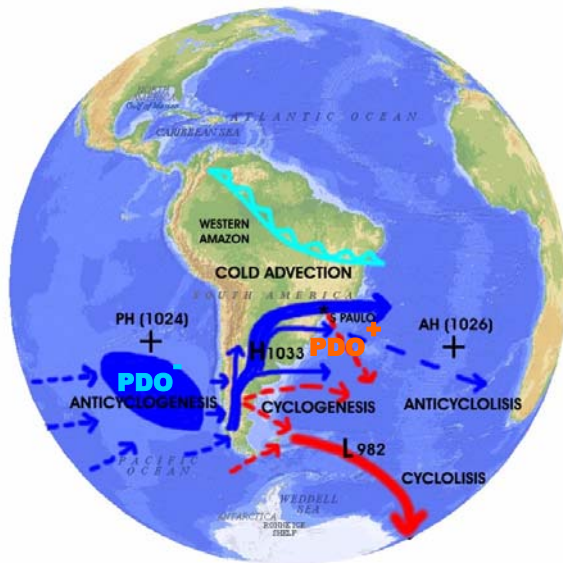


Figure 16: Conceptual model of the polar air outbreak in South America and the proposed association with the PDO phase, indicating more frequent and stronger South Pacific anticyclones further north for the negative phase (PDO⁻) and more frequent and stronger cyclones near the South Brazilian coast during the positive phase (PDO⁺). Adapted from Pezza and Ambrizzi (2005).

We are conducting further research on recent trends in several indicators of cyclone and anticyclone behavior and exploring possible physical mechanisms linking the interdecadal variability in the Pacific Ocean with mid-to-high latitude circulation, and the results will be published in the specialized literature.

3. ACKNOWLEDGMENTS

Parts of this research were funded by The University of Melbourne and the Australian Research Council (ARC).

4. REFERENCES

- Baines, P.G., 2005: Long-term variations in winter rainfall of southwest Australia and the African monsoon. *Australian Met. Mag.*, **54**, 91-102.
- Barnett, TP, Pierce, DW, Latif, M, Dommenges, D., Saravanan, R., 1999: Interdecadal interactions between the tropics and midlatitudes in the Pacific basin. *Geophys. Res. Lett.*, **26**, 615-618.
- Cane, MA, Zebiak, SE, Dolan, SC, 1986: experimental forecasts of El Nino. *Nature*, **321**, 827-832.
- Carvalho, L.M.V., Jones, C., Ambrizzi, T., 2005: Opposite phases of the antarctic oscillation and relationships with intraseasonal to interannual activity in the tropics during the austral summer. *J. Climate*, **18**, 702-718.
- Guo, Z., Bromwich, DH, Hines, KM., 2004: Modeled Antarctic precipitation. Part II: ENSO modulation over west Antarctica. *Journal of Clim.*, **17**, 448-465.
- Hoerling, MP, Kumar, A, Zhong, M, 1997: El Nino, La Nina, and the nonlinearity of their teleconnections. *J. Climate*, **10**, 1769-1786.
- Jones, DA, Simmonds, I 1993: A climatology of Southern Hemisphere extratropical cyclones. *Climate Dyn.*, **9**, 131 –145.
- Karoly, DJ, 1989: Southern Hemisphere circulation features associated with El Nino - Southern Oscillation events. *Journal of Climate*, **2**, 1239-1252.
- _____, Hope, P., Jones, PD, 1996: Decadal variations of the Southern Hemisphere circulation. *Int. J. Clim.*, **16**, 723-738.

- Latif, M. and Barnett, T.P., 1994: Causes of decadal climate variability over the North Pacific and North America. *Science*, **266**, 634-637.
- Latif, M. and Barnett, T.P., 1996: Decadal climate variability over the north Pacific and North America: Dynamics and predictability. *J. Climate*, **9**, 2407-2423.
- Mantua, NJ, Hare, SR, Zhang, Y, Wallace, JM, Francis, RC, 1997: A Pacific Interdecadal Climate Oscillation with Impacts on Salmon Production. *Bulletin of the Am. Met. Soc.*, **78**, 1069-1079.
- Meneguini, B., Simmonds, I., Smith, I., 2006: Association between Australian rainfall and the Southern Annular Mode. *Int. Journal of Climatology*, in press.
- Murray, R. J., and I. Simmonds, 1991a: A numerical scheme for tracking cyclone centres from digital data. Part I: Development and operation of the scheme. *Aust. Meteorol. Mag.*, **39**, 155-166.
- _____, and _____, 1991b: A numerical scheme for tracking cyclone centres from digital data. Part II: Application to January and July general circulation model simulations. *Aust. Meteorol. Mag.*, **39**, 167-180.
- Pezza, A.B., and Ambrizzi, T., 2003: Variability of Southern Hemisphere Cyclone and Anticyclone Behavior: Further Analysis. *J. Climate*, **16**, 1075-1083.
- Pezza, A.B., and T. Ambrizzi, 2005: Dynamical Conditions and Synoptic Tracks Associated with Different Types of Cold Surges Over Tropical South America. *International Journal of Climatology*, **25**, 215-241.
- Philander, SGH, 1985: El Nino and La Nina. *J. Atmos. Sci.*, **42**, 2652-2662.
- Rasmusson, EM, Carpenter, TH, 1982: Variations in tropical sea surface temperature and surface wind fields associated with the Southern Oscillation/El Nino. *Mon. Wea. Rev.*, **110**, 354-384.
- Renwick, J.A., 1998: ENSO-related variability in the frequency of South Pacific blocking. *Monthly Weather Review*, **126**, 3117-3123.
- Ropelewski, CF, Halpert, MS, 1989: precipitation patterns associated with the high index phase of the Southern Oscillation. *J. Climate*, **2**, 268-284.
- Rusticucci, M., Vargas, W., 2002: Cold and warm events over Argentina and their relationship with the ENSO phases: Risk evaluation analysis. *Int. Journal of Climatology*, **22**, 467-483.
- Simmonds, I., R.J. Murray and R. M. Leighton, 1999: A refinement of cyclone tracking methods with data from FROST. *Aust. Met. Mag.*, special edition, 35-49.
- Simmonds, I., and K. Keay, 2000a: Variability of Southern Hemisphere Extratropical Cyclone Behavior, 1958 – 1997. *J. Climate*, **13**, 550 – 561.
- _____, and _____, 2000b: Mean Southern extratropical cyclone behavior in the 40-year NCEP-NCAR reanalysis. *J. Climate*, **13**, 873-885.
- Simmonds, I, Keay, K, Lim, E, 2003: Synoptic activity in the seas around Antarctica. *Monthly Weather Review*, **131**, 272-288.
- Smith, SR, Stearns, CR, 1993: Antarctic pressure and temperature anomalies surrounding the minimum

in the southern Oscillation index. *Journal of Geophysical Research*, **98**, 13071-13083.

Tomita, T, Wang, B, Yasunari, T, Nakamura, H, 2001: Global patterns of decadal – scale variability observed in sea surface temperature and lower-tropospheric circulation fields. *Geophys. Res. Lett.* **106**, 805-815.

Uppala, SM., Kallberg, PW, Simmons, AJ, et al, 2005: The ERA-40 Reanalysis. *Q.J.R. Meteorol. Soc.*, **131**, 2961-3012.

Wilks, D. S., 1995: Statistical Methods in the Atmospheric Sciences. *International Geophysics Series*, **59**. Academic Press, New York, 467 pp.

Yasunaka, S., Hanawa, K., 2005: Regime shift in the global sea-surface temperatures: its relation to El Nino – Southern Oscillation events and dominant variation modes. *Int. J. Clim.*, **25**, 913-930. Doi: 10.1002/joc.1172

Zhang, Y., Wallace, J.M., Battisti, D.S., 1997: ENSO-like interdecadal variability: 1900-93. *J. Climate*, **10**, 1004-1020.